Inflammation Protein SAA2.2 Spontaneously Forms Marginally Stable Amyloid Fibrils at Physiological Temperature

ARTICLE *in* BIOCHEMISTRY · SEPTEMBER 2011

Impact Factor: 3.02 · DOI: 10.1021/bi200856v · Source: PubMed

7 AUTHORS, INCLUDING:

Zhuqiu Ye
Pharmaceutical Product Development, Rich…
7 PUBLICATIONS **59** CITATIONS
SEE PROFILE

Diane Bayron-Poueymiroy
Johns Hopkins University-CDI Labs
2 PUBLICATIONS **48** CITATIONS
SEE PROFILE

Saipraveen Srinivasan
University of Texas Southwestern Medical Ce…
12 PUBLICATIONS **94** CITATIONS
SEE PROFILE

Wilfredo Colón
Rensselaer Polytechnic Institute
62 PUBLICATIONS **2,826** CITATIONS
SEE PROFILE

Published in final edited form as:
Biochemistry. 2011 November 1; 50(43): 9184–9191. doi:10.1021/bi200856v.

Inflammation protein SAA2.2 spontaneously forms marginally stable amyloid fibrils at physiological temperature†

Zhuqiu Ye[1], **Diane Bayron**[2], **J. Javier Aguilera**[1], **Saipraveen Srinivasan**[1], **Yun Wang**[1], **Louise C. Serpell**[3], and **Wilfredo Colón**[1,*]

[1]Department of Chemistry and Chemical Biology, and Center for Biotechnology and Interdisciplinary Studies, Rensselaer Polytechnic Institute, Troy, New York 12180

[2]Department of Biology, University of Puerto Rico at Mayagüez, Calle Post, Mayagüez, PR 00681-9000

[3]School of Life Sciences, University of Sussex, Falmer, East Sussex, BN1 9QG, United Kingdom

Abstract

For nearly four decades, the formation of amyloid fibrils by the inflammation-related protein serum amyloid A (SAA) has been pathologically linked to the disease amyloid A (AA) amyloidosis. However, here we show that the non-pathogenic murine SAA2.2 spontaneously forms marginally stable amyloid fibrils at 37 °C that exhibit cross-beta structure, binding to thioflavin T, and fibrillation by a nucleation-dependent seeding mechanism. In contrast to the high stability of most known amyloid fibrils to thermal and chemical denaturation, experiments monitored by glutaraldehyde cross-linking/SDS-PAGE, thioflavin T fluorescence, and light scattering (OD_{600}) showed that the mature amyloid fibrils of SAA2.2 dissociate upon incubation in > 1.0 M urea or > 45 °C. When considering the non-pathogenic nature of SAA2.2 and its ~1000-fold increased concentration in plasma during an inflammatory response, its extreme *in vitro* amyloidogenicity under physiological-like conditions suggest that SAA amyloid might play a functional role during inflammation. Of general significance, the combination of methods used here are convenient for exploring the stability of amyloid fibrils that are sensitive to urea and temperature. Furthermore, our studies imply that analogous to globular proteins, which can possess structures ranging from intrinsically disordered to extremely stable, amyloid fibrils formed *in vivo* might have a broader range of stabilities than previously appreciated with profound functional and pathological implications

Keywords

serum amyloid A; intrinsically disordered; protein folding; amyloid stability; reactive amyloidosis; acute phase reaction

The aggregation of proteins into amyloid fibrils has been linked to a number of protein misfolding diseases, such as Alzheimer's, Parkinson's, type II diabetes, and prion disorders (1). Although originally identified as a potentially pathological protein aggregate, the observation that many structurally diverse proteins can be induced to form amyloid fibrils suggests that they are a generally accessible type of protein structure (2). The common

†This work was supported by grant NIH (R01 AG028158) to W. C.

*To whom correspondence should be addressed: Department of Chemistry and Chemical Biology, and Center for Biotechnology and Interdisciplinary Studies, Rensselaer Polytechnic Institute, Troy, New York 12180. Telephone: (518) 276-2515. Fax: (518) 276-4887. colonw@rpi.edu.

occurrence of amyloid fibrils in nature is further supported by growing evidence that they are involved in a wide range of biological functions (3–5). To date, over a dozen functional amyloids have been identified in organisms ranging from bacteria to mammals, and the number is likely to grow significantly (4). Therefore, despite their common characteristics, including fibrillar morphology, cross-β-sheet structure, high binding affinity to thioflavin T (ThT)1, and aggregation by a seeding mechanism, the functional diversity of amyloid fibrils suggests that they might have a greater range of stability than previously appreciated.

It has been shown that disease-related amyloid fibrils are usually very resistant to denaturants, often requiring harsh solvent conditions for their complete dissociation (6–10). Perhaps the best example of hyper-stable fibrils are those formed by insulin and the Ure2p prion protein, which require over 100 °C for their complete dissociation (11, 12). A recent study showed that a series of amyloid fibrils from different proteins and peptides are more thermodynamically stable than the precursor protein (13), supporting the long-standing assumption that amyloid fibrils are more stable than globular proteins and exist in an energy minimum of the folding energy landscape (8, 14). Thus, it appears that globular proteins are generally metastable in relation to amyloid fibrils (13). Indeed, the most common method for inducing globular proteins to form amyloid fibrils involves using low pH, high temperature, or modest concentrations of denaturants, resulting in fibrils that are biased towards higher stability. However, there are cases where fibrils seem to be metastable. A notable example is A-beta fibrils, which dissociate via monomer release when the concentration of A-beta is lowered below the critical monomer concentration for fibrillation (15). It has also been shown that huntingtin-exon 1 fibrils formed at 4 °C are more thermolabile and susceptible to mechanical shear (16). Other studies have shown that some amyloid fibrils, including those formed by beta microglobulin (17), lysozyme (18), and an N47A mutant of the alpha spectrin SH3 domain (19) have sensitivities to denaturants that are similar to those exhibited by globular proteins. Therefore, it seems that the high stability often observed for amyloid fibrils formed *in vitro*, might not accurately represent the range of amyloid stability that might exist in nature.

In this study, we probed the resistance towards thermal and chemical denaturation of mature amyloid fibrils formed by mice serum amyloid A (SAA) 2.2 under physiologically relevant conditions. SAA is a major class of acute phase reactant proteins, and its concentration in serum increases up to 1000-fold upon a pro-inflammatory stimuli (20, 21). It is well known that persistently high levels of SAA during chronic inflammatory disease (e.g. rheumatoid arthritis) or recurrent acute response (e.g. tuberculosis) can occasionally result in amyloid A (AA) amyloidosis (also known as reactive amyloidosis), a disease in which mainly N-terminal fragments of SAA form amyloid deposits in various organs (22). In mouse models of AA amyloidosis, a dramatic increase in the expression of SAA2.1 and SAA1.1 isoforms occurs in mice exposed to inflammatory reagents (21, 23), but the latter predominate in the amyloid deposits (24). The CE/J mouse strain only produces the SAA2.2 isoform, and it was found to be nonpathogenic (25, 26). Interestingly, although SAA2.2 is non-pathogenic *in vivo*, we have previously shown that it is an extremely amyloidogenic protein, spontaneously forming fibrils *in vitro* at 37 °C and pH 7.4 (27). Here, the amyloid nature of mature SAA2.2 fibrils was further characterized and their stability was probed by exposing them to a range of temperatures or urea concentrations. Our results show that SAA2.2 amyloid fibrils formed at 37°C, and at SAA concentrations that mimic an inflammatory response, were denatured at modest temperature and urea concentration that would be tolerated by most globular proteins. The marginal stability of SAA2.2 fibrils has

[1]Abbreviations: SAA, Serum amyloid A; AA, amyloid A; AFM, atomic force microscopy; ThT, thioflavin T; Far UV, far ultra-violet; CD, circular dichroism; SDS, sodium dodecyl sulfate; GCL, Glutaraldehyde cross-linking; SDS-PAGE, sodium dodecyl sulfate - polyacrylamide gel electrophoresis; GuHCl; DMSO, dimethylsulfoxide; OD_{600}, optical density at 600nm

implications for SAA function, and suggests that amyloid fibrils formed *in vivo* might possess a wide range of intrinsic stability.

EXPERIMENTAL PROCEDURES

SAA2.2 Expression/Purification and Preparation of SAA2.2 fibrils

The murine SAA2.2 cDNA was ligated into a pET21-a(+) vector between the Nde1 and BamH1 sites and transformed into *E. coli* strain BL21 (DE3) pLysS competent cells as previously described (28). SAA2.2 expression and purification was done as previously described (29). The refolding of SAA2.2 hexamer was achieved by dialyzing SAA2.2 (1–2 mg/ml, in 6 M urea) against 20 mM Tris-HCl buffer (pH 8.0) in the cold room overnight followed by storing at 4°C over a week. The SAA2.2 sample was then transferred to a vial, and after adjusting the pH to 7.4, it was incubated at 37 °C without agitation for 2–3 weeks to make mature SAA2.2 fibrils. The fibrils were stored at 4°C with 0.02% NaN_3.

Atomic Force Microscopy (AFM)

A 20 μL aliquot of fibril solution was diluted 20-fold to ~0.1 mg/mL, applied to a freshly cleaved mica surface and incubated for 15 min, and then gently rinsed with 2–3 mL MilliQ water to remove the extra fibril layers. Excess water was dried with nitrogen flow for 5 min before imaging. AFM images were obtained at RT using a MFP-3D™ atomic force microscope from Asylum Research (Santa Barbara, CA), operating in tapping mode in air. Si cantilevers (AC240TS, Olympus) with a spring constant of 2 N/m and tip radius less than 10 nm were used. Image analysis was performed with the Igor Pro 5.0 image-processing package (WaveMetrics, Inc., Portland, OR).

Circular Dichroism (CD)

Far-UV CD spectra were recorded using an OLIS CD instrument (Bogart, Georgia). Solution of 0.1 mg/mL of SAA2.2 fibrils or SAA2.2 hexamer was prepared in 20 mM PB buffer (pH 7.4) in a 10 mm quartz cell. The wavelength spectra were collected from 190 to 260 nm at 20 C with a bandwidth of 1nm and a time constant of 1.0 sec. The data represent averages of six consecutive scans, after buffer baseline subtraction at 255 nm.

X-Ray Diffraction

A droplet SAA amyloid fibril solution (0.1 – 0.2 mg/mL) was placed between two wax filled capillary tubes arranged less than 1 mm apart and the solution was allowed to dry to form a partially aligned fibril sample as previously described (30). X-ray diffraction data was collected using a Rigaku rotating anode (CuKalpha) and RAxis 4++ detector with specimen to detector distance of 160 cm and exposure times of 10–20 min. X-ray diffraction patterns were examined using the CCP4 program, Mosflm (31)

Thioflavin T (ThT) Binding Assay

Pre-formed SAA2.2 fibril solutions were diluted with filtered Tris-HCl buffer (pH 7.4) to a final concentration of 0.1 – 0.2 mg/mL and incubated at the relevant temperature. For thermal stability experiments, a vial of 1 mL diluted fibril suspensions was incubated at different temperatures (20–85 °C) for 30 min. At each temperature point, aliquots of 30 μL of the diluted fibril suspension were mixed with 340 μL of 50 mM Glycine-NaOH buffer (pH 8.5), and 30 μL of 100 μM ThT (Sigma) in a quartz cell (10 mm pathlength) to a total volume of 400 μL. The sample was then excited at 440 nm and a 60 sec time scan of the ThT fluorescence at 485 nm was recorded at 20 °C using a F-4500 Hitachi (Danbury, CT) fluorescence spectrophotometer. The slit lengths were set at 5.0 nm for excitation and 10 nm for emission. A working fibril suspension with absolute unit of ThT fluorescence signal

around 100 AU was designed in each experiment to ensure a constant fibril concentration during ThT fluorescence measurements. Fibrils were concentrated by spinning down at 5000 rpm for 1 min, removing some of supernatant, and re-suspending the fibrils.

Glutaraldehyde Cross-linking (GCL)/SDS-PAGE to Monitor Fibril Denaturation

Aliquots of 30 μL SAA2.2 fibrils (0.1 – 0.2 mg/mL) were incubated at various temperatures or concentrations of urea for 30 and 10 min, respectively. Each aliquot was incubated for 10 min in 0.7% (v/v, final concentration) glutaraldehyde (Sigma), and the cross-linking reaction was quenched by adding Tris-HCl (pH 6.8) to a final concentration of 0.1 M. The cross-linked samples were then analyzed by 14% SDS-PAGE, and the gel bands were quantified via ImageQuant TL (v2003, Amersham Biosciences Ltd, UK).

Light Scattering

After incubating the SAA2.2 fibrils (0.1 – 0.2 mg/mL) at different concentrations of urea for 10 min, the stability of SAA2.2 fibrils to urea was determined by monitoring the extent of light scattering of the fibrils at 600 nm (OD_{600}). The data was recorded for 60s and then averaged. Light scattering measurements were performed with a Hitachi fluorescence spectrophotometer, model F-4500 (Danbury, CT), at 20 °C using a quartz cell with a 10-mm light path. The excitation and emission wavelengths were both set at 600 nm, and the slit width was 5 nm and 10 nm for the excitation and emission, respectively.

RESULTS

SAA2.2 Characterization of Amyloid Fibrils Formed Spontaneously Under Physiological-like Conditions

Atomic force microscopy (AFM) of SAA2.2 samples incubated for 2 weeks at 37 °C and pH 7.4 revealed mature fibrils (Figure 1a) that exhibited lateral self-association (Figure 1b). Large oligomers and short protofibrils were also clearly seen (Figure 1b). The SAA2.2 fibrils showed a height of 1–2 nm, but the actual width is uncertain because fibrils imaged by AFM are significantly broadened due to effects related to the width of the AFM tip. The increase of ThT fluorescence upon binding to ordered β-sheet aggregates is widely used to monitor the time course of amyloid fibril formation (32). The fibrillation kinetics of SAA2.2 monitored by ThT fluorescence exhibited a concentration-dependent lag phase (Figure 2), consistent with the nucleation/seeding mechanism observed for the amyloid formation of many proteins and peptides. Since native SAA2.2 has mostly α-helical structure and little (< 10%) β-sheet content (29), we probed the secondary structure of the SAA2.2 fibrils by far-UV circular dichroism (CD). The CD spectrum of the fibrils showed minimum and maximum bands at 218 and 195 nm, respectively, consistent with a significant content of β-sheet structure (Figure 3a) (33).

The most robust test for confirming the amyloid-nature of fibrils is the presence of cross-beta structure, as determined by meridian and equatorial spacings at 4.76 and 10.6 Å, correspondingly, in X-ray diffraction experiments (34). Therefore, the diffraction pattern for SAA2.2 fibrils was obtained and two major diffraction bands were observed with a very sharp, intense signal at 4.66 Å on the meridian parallel to the fibril axis), and a very diffuse signal centered at 10.3 Å (Figure 3b) (35). A weak diffraction signal was also observed at around 3.7 Å. Together, the AFM images, the ThT fluorescence profile, the CD spectrum, and the X-ray diffraction pattern confirmed that the fibrils formed by SAA2.2 under mild conditions meet the criteria of genuine amyloid fibrils.

Amyloid Fibrils of SAA2.2 are Marginally Stable

Amyloid fibrils are commonly resistant to harsh conditions, such as SDS, urea, and high temperature, that would denature most proteins (8). However, SAA2.2 fibrils are fully denatured to the monomer when incubated in SDS, suggesting that SAA2.2 fibrils might be less stable than expected. This led us to probe their resistance to temperature and urea, as these are common protein denaturants that often cannot fully denature amyloid fibrils. We incubated 0.1 – 0.2 mg/mL samples of SAA2.2 fibrils at different temperatures for 30 min and then used glutaraldehyde cross-linking (GCL)/SDS-PAGE to trap the various species (from fibrils to the monomer) present, and thereby monitor the extent of fibril and oligomer dissociation. When SAA2.2 fibrils were crossed-linked at RT, they could not enter the resolving gel and only a faint monomer band was observed in SDS-PA GE (Figure 4a). However, as the incubation temperature was increased above 37 °C, the fibrils began to dissociate and the density of the monomer band increased, demonstrating that the SAA2.2 fibrils are sensitive to modest temperature, and therefore are marginally stable at physiological temperature (Figure 4a). The gel data was then imaged and the relative density of the monomer band against temperature was plotted, resulting in a fibril denaturation transition with a midpoint of ~58 °C (Figure 4b). In parallel, the loss of ThT fluorescence was also used to monitor the temperature-induced denaturation of SAA2.2 fibrils, and the decrease in fluorescence follows a sigmoidal transition with a midpoint of ~48 °C (Figure 4b). Interestingly, comparison of the GCL/SDS-PAGE and ThT data show that the loss of ThT fluorescence precedes the appearance of SAA2.2 monomer in the gel. This suggests that the mature SAA2.2 fibrils first dissociated to large oligomers or protofibrils with reduced ThT binding before further denaturing to the monomer.

To further confirm the fragility of SAA2.2 fibrils, we incubated them in different concentrations of urea and monitored the denaturation transition using GCL/SDS-PAGE and turbidity/light scattering measurements at 600 nm (OD_{600}). We used turbidity instead of ThT fluorescence because the latter was not very reproducible, perhaps due to the effect of urea on the fluorescence of ThT. The fibrils were incubated in urea for 10 min and then cross-linked with glutaraldehyde for 10 min followed by SDS-PAGE (Figure 5a). The density of the monomer bands was then analyzed and plotted against the concentration of urea (Figure 5b), yielding a sigmoidal transition with a midpoint of ~1.4 M. A similar transition was observed upon incubation for 30 min, suggesting that equilibrium had been reached after 10 min. Despite the absence of oligomer in the running gel, it is likely that fibril fragmentation occurs as the concentration of urea is increased.

The OD_{600} signal of the same fibril samples analyzed by GCL/SDS-PAGE decreased at lower concentrations of urea than the appearance of the SAA2.2 monomer in the gel (Figure 5), indicating that the fibrils dissociated to intermediate species that scattered less light. Figure 5b shows the transition curve obtained from turbidity measurements, as well as the GCL/SDS-PAGE data for comparison. The turbidity of the SAA2.2 fibril sample began to decrease even at the lowest concentrations (0.3 M) of urea and exhibited a transition midpoint of ~1.0 M; the transition was completed by ~2.0 M urea. Similar to the thermal denaturation experiment where the ThT and GCL/SDS-PAGE data had different T_m values, the urea denaturation of the fibrils monitored by turbidity exhibited a lower transition midpoint (1.0) than that obtained (1.4 M) by GCL/SDS-PAGE. This supports the interpretation that the SAA2.2 fibrils first fragment into pre-fibrillar intermediate species that do not bind ThT and scatter less light at 600 nm. Since these pre-fibrillar species do not enter the gel, they must be large oligomers and/or protofibrils, perhaps like those seen in Figure 1. Therefore, we incubated mature SAA2.2 fibrils for 30 min at 50 °C, which is near their denaturation midpoint monitored by ThT (Figure 4b), and analyzed the structure of the fibrils by AFM (Figure 6). As a control, the same sample was first incubated at 37 °C before raising the temperature further, and analyzed by AFM to confirm the presence of mature

fibrils (Figure 6a). Figure 6b shows that the SAA2.2 amyloid fibrils incubated at 50 °C indeed first dissociate to short fibrils and large oligomers before denaturing to the monomer.

DISCUSSION

Exploring the Stability of SAA2.2 Fibrils Using GCL/SDS-PAGE

In contrast to amyloid fibrils from beta microglobulin (36), lysozyme (18), transthyretin (37), SH3 domain (19), Ure2p prion (12), and insulin (11), which require much higher temperature – in some cases 100 °C or higher (11, 12) – for their complete denaturation, we showed that SAA2.2 fibrils undergo fragmentation and dissociation under modest denaturing conditions. After incubation at different temperatures or concentrations of urea we used GCL to block the remaining fibrils and/or oligomers from dissociating upon exposure to SDS. GCL also trapped the monomeric SAA2.2 present, thereby preventing them from re-aggregating. This simple approach allowed us to monitor the dissociation of the fibrils at significantly lower urea concentration and temperatures, in contrast to other amyloid fibrils that are hyper-resistant to denaturants (11, 12) or have denaturant sensitivities that are comparable with globular proteins (11, 18, 19, 36). Thus, to the best of our knowledge, the amyloid fibrils formed by SAA2.2 at 37 °C are among the least stable observed for any protein or peptide. It should be noted that because the denaturation of the fibrils is a complex process involving fibril fragmentation into different species, the transition midpoint values obtained might not represent true fibril-monomer equilibrium parameters. In contrast to A-beta fibrils, which are in dynamic equilibrium with the monomer, and appear to break down via monomer dissociation (11, 12), our denaturation (Figures 4 and 5) and AFM (Figure 6) data suggest that SAA2.2 fibrils first fragment into mostly short fibrils, protofibrils, and large oligomers. This is similar to the fragmentation of fibrils observed in yeast prion models, where generation of new seeds for further polymerization determines the strength of the prion phenotype. (38). Thus, the SAA2.2 fibrils are less resistant to heat and urea than the oligomeric fibril precursors. This is consistent with the observation that the formation of fibrils is preceded by the obligatory formation of spherical or rod shaped oligomers (39, 40) that are in equilibrium with monomers and full-length fibrils. Schmit et. al. have suggested that denaturants weaken hydrophobic and hydrogen-bonding interactions, thus disrupting aggregation and shifting the equilibrium towards oligomers (41) .

Biological and Pathological Implications of the Marginal Stability of SAA2.2 Amyloid Fibrils

A remarkable feature of SAA is that during inflammation its concentration can increase within 24 hrs up to 1000-fold and 1 mg/mL (20, 21, 42). It is known that just as the concentration of SAA quickly rises upon an inflammatory insult, it can quickly decrease to normal levels (42). This efficient regulation of SAA concentration is consistent with its intrinsically disordered structure and the marginal stability of the SAA oligomers observed *in vitro* (27). Although the acute phase response is part of the innate immune defense system, the biological function of SAA that requires this dramatic increase in protein expression remains poorly understood. SAA2.2's ability to spontaneously form marginally stable amyloid fibrils *in vitro* at 37 °C at the high SAA concentrations (0.1 – 1.0 mg/mL) present during inflammation, together with the growing evidence that amyloid fibrils can have diverse functional roles *4, 5*), make it conceivable that SAA amyloid might serve a functional role.

The formation of amyloid by SAA has been linked to AA amyloidosis for ~ 40 years since the N-terminal 76 residues of SAA was found in clinical amyloid deposits, as a secondary effect to chronic inflammatory disease (21). In mice, induction of an inflammatory response

results in amyloid deposition of SAA1.1; however, it is remarkable that even though SAA2.2 is non-pathogenic in mice, it is highly amyloidogenic *in vitro* (20, 23). Since AA amyloidosis occurs in only 5–10% of humans during persistent chronic inflammatory conditions (20), the possibility that SAA amyloid formation might be an inherent property of SAA proteins needs to be further explored. Although it is not clear why some individuals develop AA amyloidosis or why SAA2.2 is not pathogenic in mice, it is plausible that the amyloid fibril deposits in organs might be stable and more difficult to degrade. Studies of AA fibrils extracted from murine spleen and liver showed resistance to high hydrostatic pressure, and the fibrils were only partially dissociated at high temperature (43). Pathological SAA fibrils might be more stable than the fibrils formed *in vitro* via binding to serum amyloid P or glycosaminoglycans, which are known to stabilize amyloid fibrils (44). SAA is an extremely conserved protein in all vertebrates, so it will be interesting to explore whether SAA proteins, pathogenic and non-pathogenic, from different species also spontaneously form marginally stable amyloid fibrils at 37 °C.

Do Amyloid Fibrils Formed In Vivo Have a Broad Range of Stability?

The formation of amyloid fibrils *in vitro* by most globular proteins often require destabilizing conditions, such as acidic pH, chemical denaturants, or increase in temperature (8, 45). Interestingly, it has been shown that depending on the solvent conditions, peptides and proteins can often form different morphological structures of variable stabilities (46–48). This polymorphic potential of fibrils explains why harsh non-physiological conditions select against the formation of unstable amyloid fibrils. This overrepresentation of stable fibrils in the literature might have contributed to the perception that amyloid fibrils are intrinsically very stable structures. Our results show that amyloid fibrils formed under mild conditions (i.e. 37 °C, pH 7.4) might select for amyloid structures that are marginally stable, as evidenced by their disruption at temperatures > 40 °C and [urea] > 0.1 M. It would be interesting to compare the stability of amyloid fibrils formed by different proteins under physiological-like conditions to determine the range of their sensitivity to denaturants, as well as their thermodynamic and kinetic stabilities. It seems probable that the stability of amyloid fibrils might vary significantly depending on the type and extent of molecular interactions present within and between fibrils (35, 49–51).

The growing evidence that amyloid fibrils carry out a variety of biological functions (4, 5), suggests that some functions might not be compatible with highly stable fibrils, as this would interfere with their regulation and degradation. A remarkable example of physiological regulation mediated by amyloid fibrils is the case of peptide hormones, which aggregate into amyloid fibrils for storage in secretory granules and releases the functional peptide as needed (52). A-beta fibrils are another example of fibrils that dissociate via monomer release (15). Although we show that denaturation of SAA2.2 fibrils proceeds via fragmentation and dissociation to the monomer, it is possible that fibril stability is modulated *in vivo* to release functional monomeric or oligomeric units. However, testing this hypothesis would require probing the stability of SAA fibrils *in vivo*, including determining its critical monomer concentration for fibril formation. Thus, our results support the idea that amyloid fibrils in nature might have a broader range of stability like that of soluble proteins. For decades globular proteins were considered to fold into unique 3D structures with a narrow range of stability (53). However, it is now accepted that they can also form intrinsically disordered (54), as well as degradation-resistant kinetically stable conformations (55), where the former allows functional regulation and quick degradation, and the latter possess a much longer half-life. Similarly, amyloid fibrils in nature might possess stabilities that range from marginal to extremely high (56). Understanding the stability range of amyloid fibrils, whether intrinsic or modulated by ligand binding and the

cellular environment, will be critical for gaining a better understanding of the functional and pathological roles of amyloid stability.

Acknowledgments

We thank Peter Tessier for his useful comments of our manuscript.

REFERENCES

1. Dobson CM. The structural basis of protein folding and its links with human disease. Philos Trans R Soc Lond B Biol Sci. 2001; 356:133–145. [PubMed: 11260793]
2. Chiti F, Dobson CM. Protein misfolding, functional amyloid, and human disease. Annu Rev Biochem. 2006; 75:333–366. [PubMed: 16756495]
3. Fowler DM, Koulov AV, Balch WE, Kelly JW. Functional amyloid--from bacteria to humans. Trends Biochem Sci. 2007; 32:217–224. [PubMed: 17412596]
4. Greenwald J, Riek R. Biology of amyloid: structure, function, and regulation. Structure. 2010; 18:1244–1260. [PubMed: 20947013]
5. Maury CP. The emerging concept of functional amyloid. J Intern Med. 2009; 265:329–334. [PubMed: 19207371]
6. Knowles TP, Fitzpatrick AW, Meehan S, Mott HR, Vendruscolo M, Dobson CM, Welland ME. Role of intermolecular forces in defining material properties of protein nanofibrils. Science. 2007; 318:1900–1903. [PubMed: 18096801]
7. Knowles TP, Smith JF, Craig A, Dobson CM, Welland ME. Spatial persistence of angular correlations in amyloid fibrils. Phys Rev Lett. 2006; 96 238301.
8. Meersman F, Dobson CM. Probing the pressure-temperature stability of amyloid fibrils provides new insights into their molecular properties. Biochim Biophys Acta. 2006; 1764:452–460. [PubMed: 16337233]
9. Pepys MB. Pathogenesis, diagnosis and treatment of systemic amyloidosis. Philos Trans R Soc Lond B Biol Sci. 2001; 356:203–210. [PubMed: 11260801]
10. Smith JF, Knowles TP, Dobson CM, Macphee CE, Welland ME. Characterization of the nanoscale properties of individual amyloid fibrils. Proc Natl Acad Sci U S A. 2006; 103:15806–15811. [PubMed: 17038504]
11. Arora A, Ha C, Park CB. Insulin amyloid fibrillation at above 100 degrees C: new insights into protein folding under extreme temperatures. Protein Sci. 2004; 13:2429–2436. [PubMed: 15295111]
12. Baxa U, Ross PD, Wickner RB, Steven AC. The N-terminal prion domain of Ure2p converts from an unfolded to a thermally resistant conformation upon filament formation. J Mol Biol. 2004; 339:259–264. [PubMed: 15136031]
13. Baldwin AJ, Knowles TP, Tartaglia GG, Fitzpatrick AW, Devlin GL, Shammas SL, Waudby CA, Mossuto MF, Meehan S, Gras SL, Christodoulou J, Anthony-Cahill SJ, Barker PD, Vendruscolo M, Dobson CM. Metastability of native proteins and the phenomenon of amyloid formation. J Am Chem Soc. 2011; 133:14160–14163. [PubMed: 21650202]
14. Gazit E. The "Correctly Folded" state of proteins: is it a metastable state? Angew Chem Int Ed Engl. 2002; 41:257–259. [PubMed: 12491403]
15. O'Nuallain B, Shivaprasad S, Kheterpal I, Wetzel R. Thermodynamics of A beta(1–40) amyloid fibril elongation. Biochemistry. 2005; 44:12709–12718. [PubMed: 16171385]
16. Nekooki-Machida Y, Kurosawa M, Nukina N, Ito K, Oda T, Tanaka M. Distinct conformations of in vitro and in vivo amyloids of huntingtin-exon1 show different cytotoxicity. Proc Natl Acad Sci U S A. 2009; 106:9679–9684. [PubMed: 19487684]
17. Kardos J, Micsonai A, Pal-Gabor H, Petrik E, Graf L, Kovacs J, Lee YH, Naiki H, Goto Y. Reversible heat-induced dissociation of beta2-microglobulin amyloid fibrils. Biochemistry. 2011; 50:3211–3220. [PubMed: 21388222]

18. Mossuto MF, Dhulesia A, Devlin G, Frare E, Kumita JR, de Laureto PP, Dumoulin M, Fontana A, Dobson CM, Salvatella X. The non-core regions of human lysozyme amyloid fibrils influence cytotoxicity. J Mol Biol. 2010; 402:783–796. [PubMed: 20624399]
19. Morel B, Varela L, Conejero-Lara F. The thermodynamic stability of amyloid fibrils studied by differential scanning calorimetry. J Phys Chem B. 2010; 114:4010–4019. [PubMed: 20199038]
20. De Beer FC, Mallya RK, Fagan EA, Lanham JG, Hughes GR, Pepys MB. Serum amyloid-A protein concentration in inflammatory diseases and its relationship to the incidence of reactive systemic amyloidosis. Lancet. 1982; 2:213–234.
21. McAdam KP, Sipe JD. Murine model for human secondary amyloidosis: genetic variability of the acute-phase serum protein SAA response to endotoxins and casein. J Exp Med. 1976; 144:1121–1127. [PubMed: 978136]
22. Husebekk A, Skogen B, Husby G, Marhaug G. Transformation of amyloid precursor SAA to protein AA and incorporation in amyloid fibrils in vivo. Scand J Immunol. 1985; 21:283–287. [PubMed: 3922050]
23. Skinner M, Shirahama T, Benson MD, Cohen AS. Murine amyloid protein AA in casein-induced experimental amyloidosis. Lab. Invest. 1977; 36:420–427. [PubMed: 403374]
24. Hoffman JS, Ericsson LH, Eriksen N, Walsh KA, Benditt EP. Murine tissue amyloid protein AA: NH_2-terminal sequence identity with only one of two serum amyloid protein (apoSAA) gene product. J. Exp. Med. 1984; 159:641–646. [PubMed: 6693836]
25. de Beer MC, de Beer FC, McCubbin WD, Kay CM, Kindy MS. Structural prerequisites for serum amyloid A fibril formation. J. Biol. Chem. 1993; 268:20606–20612. [PubMed: 8376413]
26. Sipe JD, Carreras I, Gonnerman WA, Cathcart ES, de Beer MC, de Beer FC. Characterization of the inbred CE/J mouse strain as amyloid resistant. Am J Pathol. 1993; 143:1480–1485. [PubMed: 7901995]
27. Wang L, Lashuel HA, Colon W. From hexamer to amyloid: marginal stability of apolipoprotein SAA2.2 leads to in vitro fibril formation at physiological temperature. Amyloid. 2005; 12:139–148. [PubMed: 16194868]
28. Yamada T, Kluve-Beckerman B, Liepnieks JJ, Benson MD. Fibril formation from recombinant human serum amyloid A. Biochim et Biophys Acta. 1994; 1226:323–329.
29. Wang L, Lashuel HA, Walz T, Colon W. Murine apolipoprotein serum amyloid A in solution forms a hexamer containing a central channel. Proc Natl Acad Sci U S A. 2002; 99:15947–15952. [PubMed: 12456883]
30. Makin OS, Serpell LC. X-ray diffraction studies of amyloid structure. Methods Mol Biol. 2005; 299:67–80. [PubMed: 15980596]
31. Winn MD. An overview of the CCP4 project in protein crystallography: an example of a collaborative project. J Synchrotron Radiat. 2003; 10:23–25. [PubMed: 12511787]
32. Naiki H, Higuchi K, Hosokawa M, Takeda T. Fluorometric determination of amyloid fibrils in vitro using the fluorescent dye, thioflavin T1. Anal Biochem. 1989; 177:244–249. [PubMed: 2729542]
33. Reed J, Reed TA. A set of constructed type spectra for the practical estimation of peptide secondary structure from circular dichroism. Anal Biochem. 1997; 254:36–40. [PubMed: 9398343]
34. Makin OS, Serpell LC. Structures for amyloid fibrils. FEBS J. 2005; 272:5950–5961. [PubMed: 16302960]
35. Jahn TR, Makin OS, Morris KL, Marshall KE, Tian P, Sikorski P, Serpell LC. The common architecture of cross-beta amyloid. J Mol Biol. 2010; 395:717–727. [PubMed: 19781557]
36. Sasahara K, Naiki H, Goto Y. Kinetically controlled thermal response of beta2-microglobulin amyloid fibrils. J Mol Biol. 2005; 352:700–711. [PubMed: 16098535]
37. Foguel D, Suarez MC, Ferrao-Gonzales AD, Porto TC, Palmieri L, Einsiedler CM, Andrade LR, Lashuel HA, Lansbury PT, Kelly JW, Silva JL. Dissociation of amyloid fibrils of alpha-synuclein and transthyretin by pressure reveals their reversible nature and the formation of water-excluded cavities. Proc Natl Acad Sci U S A. 2003; 100:9831–9836. [PubMed: 12900507]
38. Tanaka M, Collins SR, Toyama BH, Weissman JS. The physical basis of how prion conformations determine strain phenotypes. Nature. 2006; 442:585–589. [PubMed: 16810177]

39. Krishnan R, Lindquist SL. Structural insights into a yeast prion illuminate nucleation and strain diversity. Nature. 2005; 435:765–772. [PubMed: 15944694]
40. Williamson TE, Vitalis A, Crick SL, Pappu RV. Modulation of polyglutamine conformations and dimer formation by the N-terminus of huntingtin. J Mol Biol. 2010; 396:1295–1309. [PubMed: 20026071]
41. Schmit JD, Ghosh K, Dill K. What drives amyloid molecules to assemble into oligomers and fibrils? Biophys J. 2011; 100:450–458. [PubMed: 21244841]
42. Kluve-Beckerman B, Yamada T, Hardwick J, Liepnieks JJ, Benson MD. Differential plasma clearance of murine acute-phase serum amyloid A proteins SAA1 and SAA2. Biochem J. 1997; 322(Pt 2):663–669. [PubMed: 9065791]
43. Dubois J, Ismail AA, Chan SL, Ali-Khan Z. Fourier transform infrared spectroscopic investigation of temperature- and pressure-induced disaggregation of amyloid A. Scand J Immunol. 1999; 49:376–380. [PubMed: 10219762]
44. Tennent GA, Lovat LB, Pepys MB. Serum amyloid P component prevents proteolysis of the amyloid fibrils of Alzheimer disease and systemic amyloidosis. Proc Natl Acad Sci U S A. 1995; 92:4299–4303. [PubMed: 7753801]
45. Sun Y, Makarava N, Lee CI, Laksanalamai P, Robb FT, Baskakov IV. Conformational stability of PrP amyloid fibrils controls their smallest possible fragment size. J Mol Biol. 2008; 376:1155–1167. [PubMed: 18206163]
46. Andersen CB, Hicks MR, Vetri V, Vandahl B, Rahbek-Nielsen H, Thogersen H, Thogersen IB, Enghild JJ, Serpell LC, Rischel C, Otzen DE. Glucagon fibril polymorphism reflects differences in protofilament backbone structure. J Mol Biol. 2010; 397:932–946. [PubMed: 20156459]
47. Kodali R, Wetzel R. Polymorphism in the intermediates and products of amyloid assembly. Curr Opin Struct Biol. 2007; 17:48–57. [PubMed: 17251001]
48. Kodali R, Williams AD, Chemuru S, Wetzel R. Abeta(1–40) forms five distinct amyloid structures whose beta-sheet contents and fibril stabilities are correlated. J Mol Biol. 2010; 401:503–517. [PubMed: 20600131]
49. Nelson R, Sawaya MR, Balbirnie M, Madsen AO, Riekel C, Grothe R, Eisenberg D. Structure of the cross-beta spine of amyloid-like fibrils. Nature. 2005; 435:773–778. [PubMed: 15944695]
50. Paravastu AK, Leapman RD, Yau WM, Tycko R. Molecular structural basis for polymorphism in Alzheimer's beta-amyloid fibrils. Proc Natl Acad Sci U S A. 2008; 105:18349–18354. [PubMed: 19015532]
51. Reddy G, Straub JE, Thirumalai D. Dynamics of locking of peptides onto growing amyloid fibrils. Proc Natl Acad Sci U S A. 2009; 106:11948–11953. [PubMed: 19581575]
52. Maji SK, Perrin MH, Sawaya MR, Jessberger S, Vadodaria K, Rissman RA, Singru PS, Nilsson KP, Simon R, Schubert D, Eisenberg D, Rivier J, Sawchenko P, Vale W, Riek R. Functional amyloids as natural storage of peptide hormones in pituitary secretory granules. Science. 2009; 325:328–332. [PubMed: 19541956]
53. Schellman JA. The thermodynamic stability of proteins. Annu Rev Biophys Biophys Chem. 1987; 16:115–137. [PubMed: 3297085]
54. Fink AL. Natively unfolded proteins. Curr Opin Struct Biol. 2005; 15:35–41. [PubMed: 15718131]
55. Sanchez-Ruiz JM. Protein kinetic stability. Biophys Chem. 2010; 148:1–15. [PubMed: 20199841]
56. Wiggins RC. Prion stability and infectivity in the environment. Neurochem Res. 2009; 34:158–168. [PubMed: 18483857]

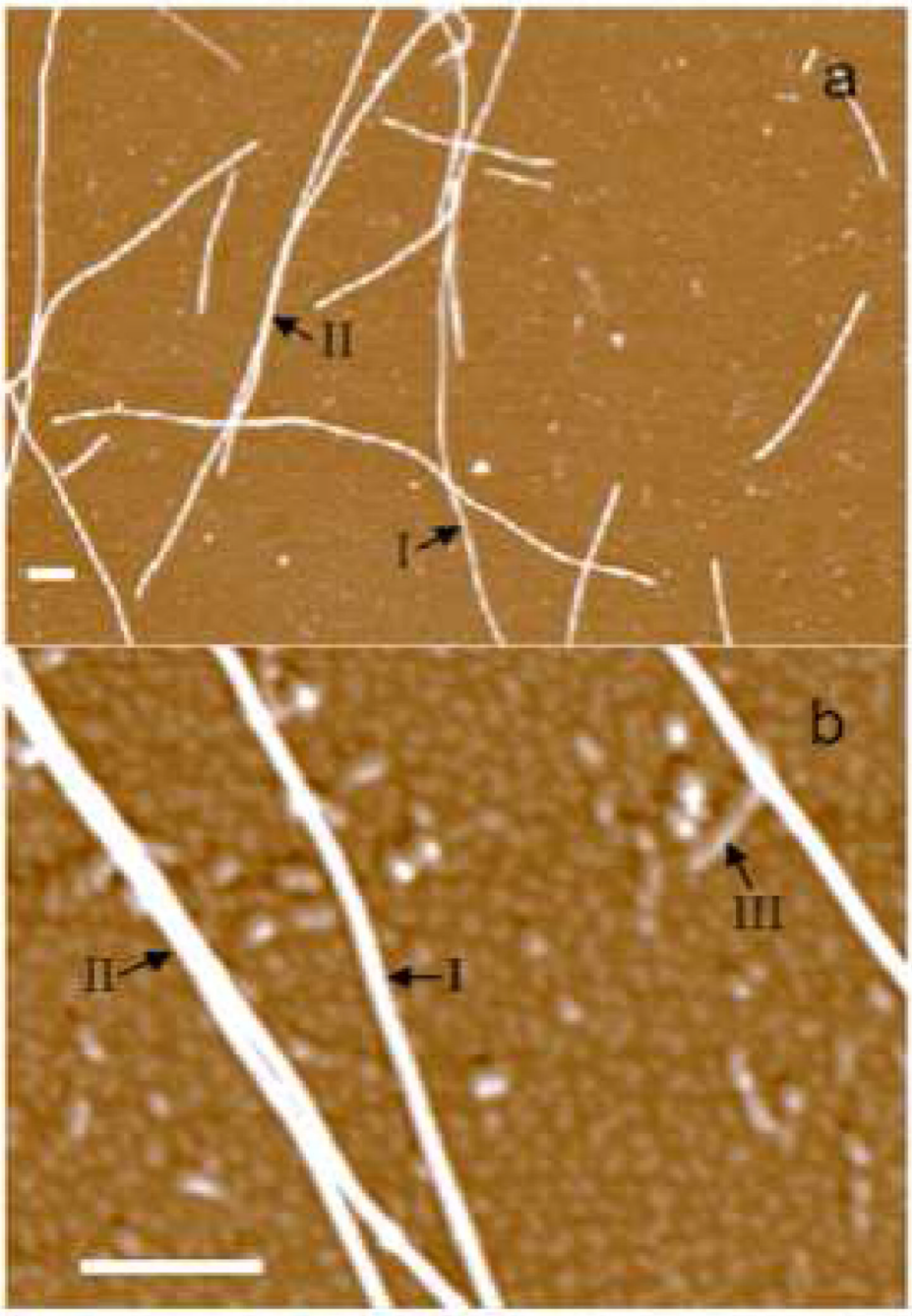

Figure 1.

AFM images of mature SAA2.2 fibrils formed after incubation of SAA2.2 (20 mM Tris-HCl, pH 7.4) at 37 °C for 2–3 weeks. Several types of structures are evident, including I) fibrils with 2 nm in height and of variable length; II) several type I fibrils joined together to form higher-ordered fibrils; and III) short protofibrils formed by interaction of spherical oligomers. Scale bars in (a) and (b) represent 500 and 200 nm, respectively.

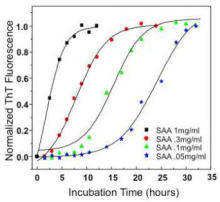

Figure 2.

The formation of SAA2.2 amyloid fibrils monitored by thioflavin T fluorescence. The curves represent the changes in ThT fluorescence as a function of time upon binding to SAA2.2 fibrils formed at different protein concentrations (20 mM Tris-HCl, pH 7.4) and 37 °C. The presence of a variable lag phase is consistent with a nucleation/seeding mechanism.

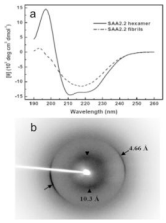

Figure 3.

(a) Far-UV CD spectrum and (b) X-ray diffraction of SAA2.2 amyloid fibrils. The CD spectrum of SAA2.2 fibrils contains a minimum at 218 nm and maximum at 195 nm, consistent with the significant presence of β-sheet structure. Both, the fibril solution and hexameric SAA2.2 were diluted to a final concentration of 0.1 mg/mL in PB buffer (pH 7.4). X-ray fibril diffraction pattern from SAA2.2 showing a classic amyloid-like cross-beta pattern with diffraction signals at 4.66 Å (arrows) and 10.3 Å (arrow heads).

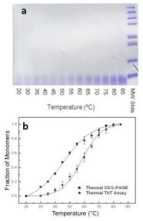

Figure 4.

Thermal stability of SAA2.2 fibrils monitored by GCL/SDS-PAGE and ThT fluorescence. (a) Representative gel showing the extent of monomer populated after cross-linking at various temperatures. (b) The gel data was analyzed by quantifying the bands and then plotting the relative fraction of SAA2.2 monomer versus temperature (■). The thermal denaturation of SAA2.2 fibrils was also monitored by the disappearance of the ThT fluorescence (●). The estimated transition midpoint for the gel and ThT data were ~58 ° and ~48 °C, respectively. Error bars are based on triplicate experiments.

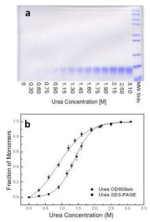

Figure 5.

Urea-induced denaturation of SAA2.2 fibrils monitored by GCL/SDS-PAGE and light scattering. (a) Representative gel data showing the extent of monomer populated after cross-linking at various concentrations of urea. (b) Gel data analyzed by plotting the density of monomer bands against urea concentrations (■). The urea-induced denaturation of SAA2.2 fibrils was also monitored by light scattering at 600 nm (●). The estimated transition midppoints for the gel and OD_{600} data were ~ 1.4 M and ~1.0 M, respectively. Error bars are based on triplicate experiments.

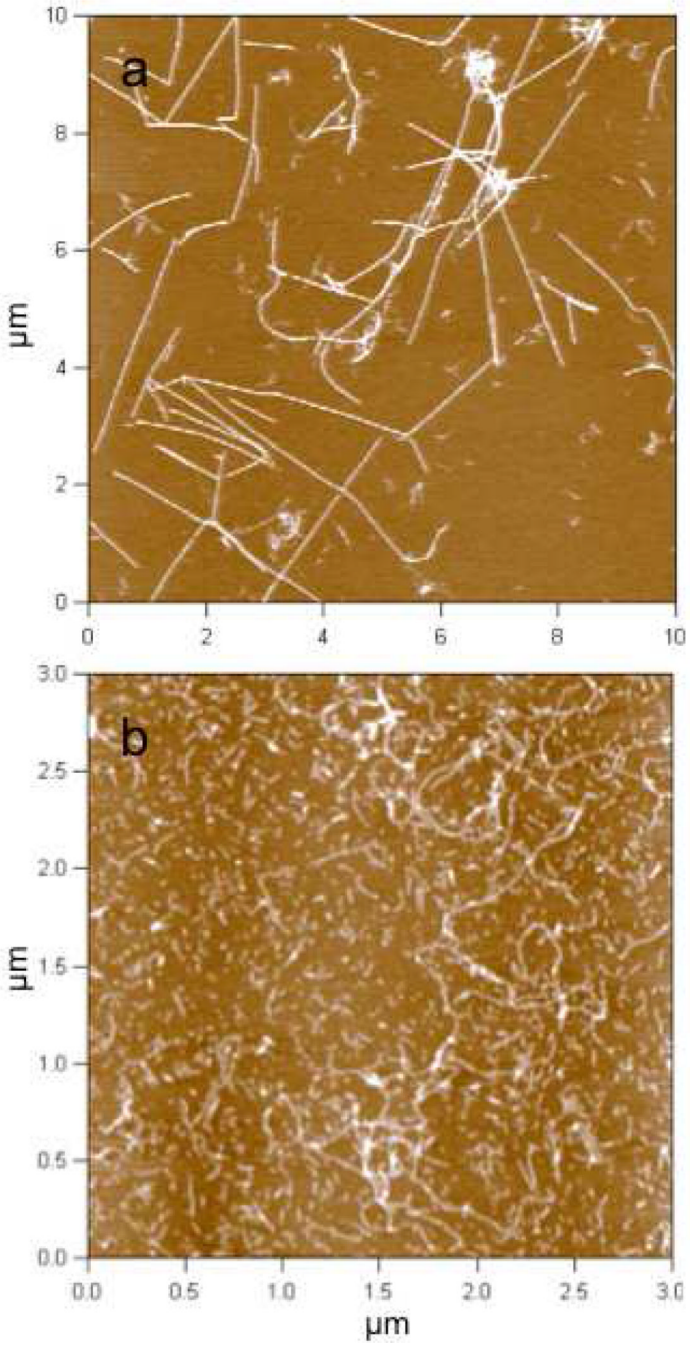

Figure 6.

Thermal denaturation of SAA2.2 amyloid fibrils examined by AFM. (a) Mature fibrils of SAA2.2 formed by incubating an SAA2.2 sample (~2.5 mg/ml in 20 mM Tris buffer, pH 7.4) at 37 °C for 2 weeks. Long fibrils interacting with each other are clearly seen before thermal denaturation. (b) Mature SAA2.2 fibrils were incubated at 40, 45 and 50 °C for 0.5 hr at each temperature in sequential order. The thermally denatured fibrils were then diluted 20 times and prepared on mica for AFM imaging in air as described in the Methods section. AFM image shows the dissociation of mature fibrils into short fibrils and protofibrils.